DOI: 10.1002/chem.200600408

Ionic Metallomesogens

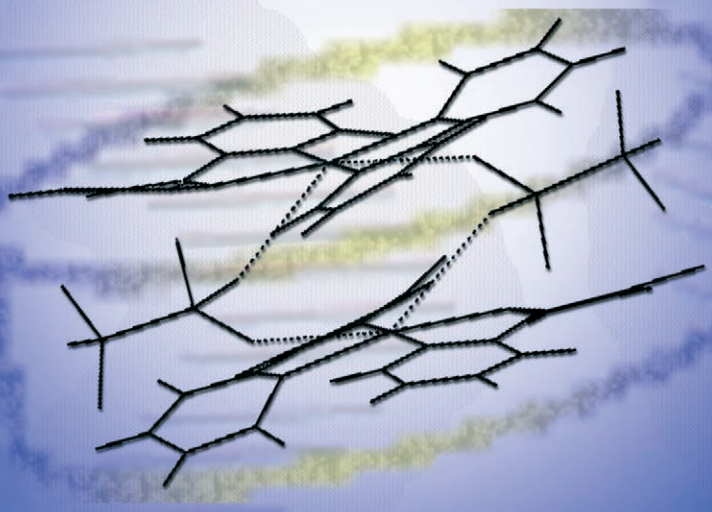

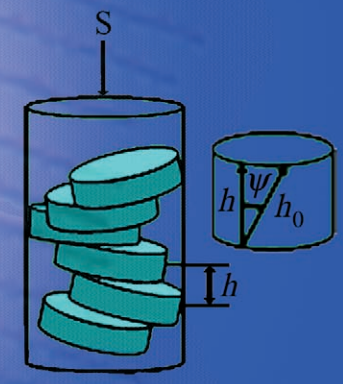

$h < h_0$
$(h = h_0 \cdot \cos\psi)$
$S_0 = S \cdot \cos\psi$

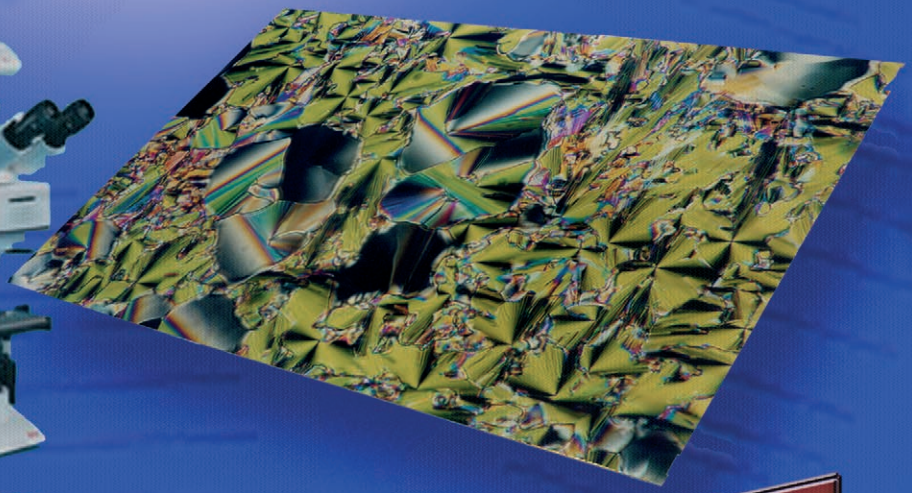

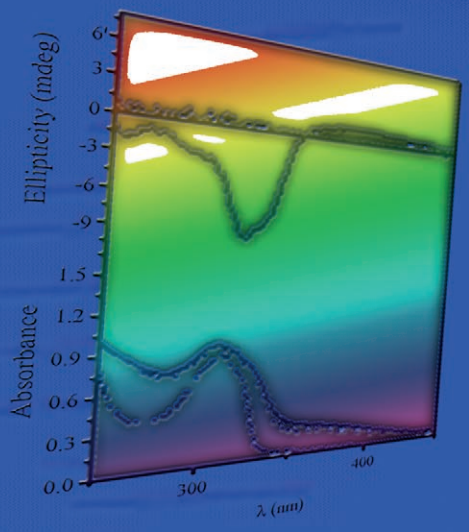

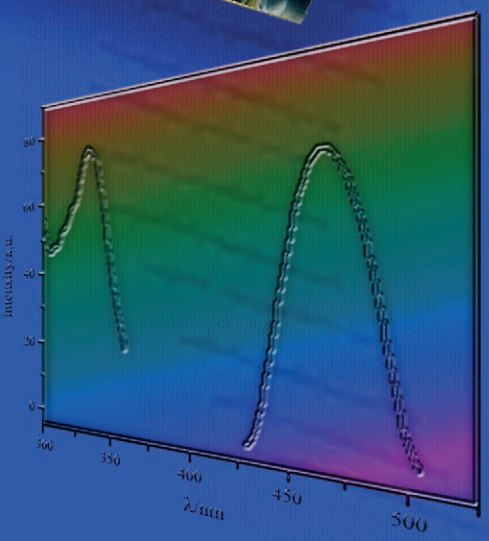

For more information see the following pages

Silver Coordination Complexes as Room-Temperature Multifunctional Materials

Daniela Pucci,*[a] Giovanna Barberio,[a] Anna Bellusci,[a] Alessandra Crispini,[a] Bertrand Donnio,[c] Loris Giorgini,[b] Mauro Ghedini,[a] Massimo La Deda,[a] and Elisabeta Ildyko Szerb[a]

Abstract: A series of bischelate ionic silver complexes $[Ag(L^*)_2][X]$ was prepared by complexation of a newly synthesized 2,2′-bipyridine containing chiral alkoxy chains in the 4,4′ positions. The appropriate choice of the construction motifs allows the preparation of new materials in which several functionalities can be introduced. Indeed, when the anion X^- is a triflate or a dodecylsulfate group, the right combination of intermolecular interactions promotes the production of liquid crystalline mesophases. Therefore, the presence of coordinating anions, which drives the supramolecular assembly, is essential to generate, at the same time, room-temperature columnar hexagonal mesomorphism, the columnar helical supramolecular structure, and excimeric emission.

Keywords: chirality · helical columnar mesophases · ionic metallomesogens · luminescence · silver

Introduction

Liquid crystals are attractive as new materials in practical device applications because of their luminescence and charge-transport properties.[1–3] Among the rich variety of structural mesomorphic species, ionic[4] and/or discotic systems are promising candidates for new applications in optoelectronics.[5–6] The incorporation of a stereogenic center within discoid mesogens may induce chiral supramolecular columnar organizations,[7] making these molecules particularly attractive for ferroelectric switching.[8–11] Moreover, the introduction of a further functionality such as a metallic reactive center, could be a good strategy for obtaining helical superstructures in columnar mesophases.[12]

Supramolecular assembly plays a key role among the possible approaches to functionalize soft materials such as liquid crystals.[13] We have recently reported on the design of metal-containing mesogens, the molecular shapes of which differ from the archetypal discogenic molecules. In these systems, the molecular organization in the mesophase is mainly driven by intermolecular attractive interactions that can induce liquid-crystalline properties regardless of the coordination geometry of the metal ion and the number of flexible chains.[14–16]

With this in mind, we aim now to extend this strategy, to develop new chiral helical superstructures in columnar mesophases, through a synthetic pathway based on several construction motifs ranging from metal coordination, π–π interactions, ionic self-assembly, stereogenic centers, and the coordinating ability of counterions.

Relevant results are described herein, in which we report the synthesis and characterization of four new ionic bischelate silver complexes $[Ag(L^*)_2][X]$ (X = BF_4^-, tetrafluoroborate, **1**; PF_6^-, hexafluorophosphate, **2**; $CF_3SO_3^-$, trifluoromethanesulfonate (triflate), OTf, **3**; and $C_{12}H_{25}OSO_3^-$, dodecylsulfate, DOS, **4**), based on a 2,2′-bipyridine ligand (L*) containing the *S*-(−)-β-citronellyl group as substituent in the 4,4′ positions. Optical microscopy, DSC, and powder X-ray

[a] Prof. D. Pucci, Dr. G. Barberio, Dr. A. Bellusci, Prof. A. Crispini, Prof. M. Ghedini, Dr. M. La Deda, Dr. E. I. Szerb
Centro di Eccellenza CEMIF.CAL-LASCAMM
CR-INSTM Unità della Calabria, Dipartimento di Chimica Università della Calabria (Italy)
E-mail: d.pucci@unical.it

[b] Dr. L. Giorgini
Unità INSTM of Bologna, Dipartimento di Chimica Industriale e dei Materiali, University of Bologna
Bologna (Italy)

[c] Dr. B. Donnio
Institut de Physique et Chimie des Matériaux de Strasbourg - Groupe des Matériaux Organiques
UMR 7504 (CNRS-Université Louis Pasteur), 23 rue du Loess
BP43, 67.034 Strasbourg cedex 2 (France)

Supporting information for this article is available on the WWW under http://www.chemeurj.org/ or from the author.

diffraction analysis have been used to characterize the liquid-crystalline behavior of the new silver derivatives. Since interesting luminescence properties have been reported for achiral $[Ag(L^n)_2]X$ complexes, at room temperature, both in solution and in the solid state,[15] the photophysical properties of complexes **1**–**4** were also investigated by using UV/Vis spectroscopy. Moreover, to evaluate the possibility of the appearance of any helical organization in the mesophase the optical activity was investigated by using circular dichroism (CD) spectroscopy.

Results and Discussion

Synthesis: As shown in Scheme 1, the chiral ligand L* was obtained through a three-step route, following the procedure previously reported for nonchiral analogous ligands.[14]

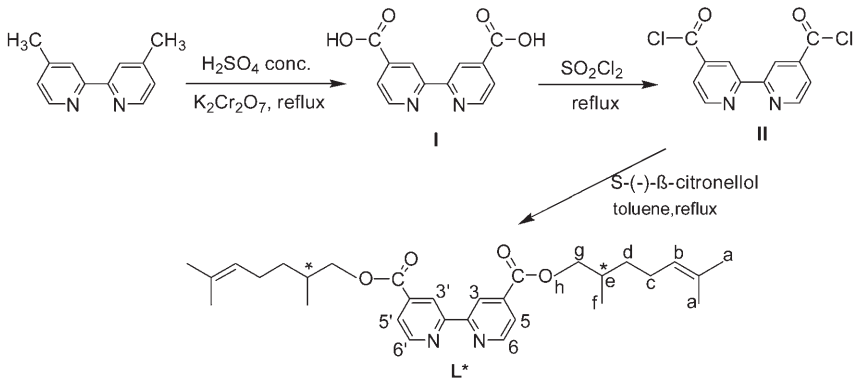

Scheme 1. Preparation of the L* ligand.

In particular, 4,4′-dimethyl-2,2′-bipyridine was oxidized to give the corresponding dicarboxylic acid **I**, which, once transformed into the more reactive diacid chloride **II** analogue,[17] reacted with the chiral alcohol *S*-(−)-β-citronellol (*S*-3,7-dimethyl-6-octen-1-ol).

Complexation of the L* ligand with several AgX salt solutions, at a 2:1 ratio, under a nitrogen atmosphere in dichloromethane, under reflux, for 24 h (Scheme 2), afforded the ionic silver complexes **1**–**4**, in good yields and of analytical purity.

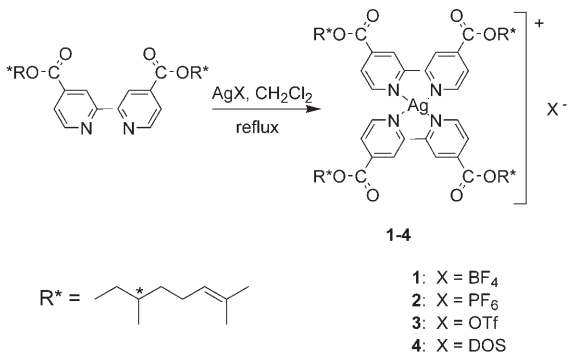

Scheme 2. Synthesis of silver complexes, $[Ag(L^*)_2][X]$, **1**–**4**.

The ionic nature of complexes **1**–**4** was confirmed by using IR spectroscopy to identify the characteristic bands of the corresponding counterions. The ^1H NMR spectra of both the free ligand and the silver complexes are very similar, but we observed a significant increase in the chemical shifts ($\Delta = 0.1$ ppm) associated with the bipyridine protons (H^3, $H^{3'}$), which are within the shielding region exerted by the ring of the complementary bipyridine.

Mesomorphism: The thermal behavior of all synthesized species was characterized by using both polarized optical microscopy (POM) and differential scanning calorimetry (DSC), while the nature of the mesophase was confirmed by using temperature-dependent powder X-ray diffraction (XRD). All thermal data are summarized in Table 1.

The thermal behavior of the $[Ag(L^*)_2][X]$ complexes was found to be strongly dependent on the nature of the counterion. The tetrafluoroborate (**1**) and the hexafluorophosphate (**2**) silver(I) complexes lack mesomorphism: At room temperature, complex **1** is an oil, whereas complex **2** is a partially crystalline solid that directly dissolves on heating without showing any sign of monotropic mesophase formation on cooling.

However, the triflate and the dodecyl sulfate derivatives (**3** and **4**, respectively) are liquid crystals already at room temperature, and exhibit large mesophase stability across a wide range of temperatures. For both complexes textures characteristic of a hexagonal columnar mesophase were observed with polarized light microscopy. The triflate derivative **3** exhibits a focal conic texture resulting from the formation of large cylindrical domains along with homeotropic zones, whereas the dodecyl sulfate derivative **4** shows mosaic and fan-shaped textures (Figure 1). DSC measurements over repeated heating–cooling cycles demonstrated that the two complexes are highly thermally stable.

Temperature-dependent powder XRD patterns confirmed that both compounds **3** and **4** exhibit a hexagonal columnar mesophase between room temperature and the temperature of the corresponding isotropic liquid. At room temperature, both X-ray diffraction patterns, as shown in Figure 2, showed a set of small-angle reflections, with a sharp and intense single peak (fundamental reflex) alongside three or four signals of lower intensity. These reflections were perfectly indexed in a hexagonal-planar symmetry with the Miller indices (10), (11), (20), (21), and (30) (Figure 2). The symmetry of the mesophase was unaffected by the counter-

Table 1. Thermal behavior of L* and $[Ag(L^*)_2][X]$ complexes and X-ray characterization of the mesomorphic complexes **3** and **4**.[a]

Compound	Transition temperatures [°C]	d_{meas} [Å]	I	Index hk	d_{calcd} [Å]	Mesophase parameters measured at 30 °C	Mesophase parameters measured at 30 °C
L*	oil						
1	oil						
2	Cr_X 60.6 I						
3	Col_h 91.0 (3.55[b]) I	21.5	vs	10	21.5		$V_{mol}=1810$ Å^3
		12.45	m	11	12.4	$a=24.8$ Å	
		10.85	m	20	10.75	$S=535$ Å^2	
		8.15	m	21	8.1	$h=3.4$ Å	
		7.1	w	30	7.15		
		7.0	br	h'			
		4.7	br	h_{ch}			
		3.55	br	h_0			
4	Col_h 56.8 (2.05[b]) I	24.2	vs	10	24.2		$V_{mol}=2110$ Å^3
		14.0	m	11	14.0	$a=28.0$ Å	
		12.1	m	20	12.1	$S=680$ Å^2	
		9.15	m	21	9.15	$h=3.1$ Å	
		7.0	br	h'			
		4.7	br	h_{ch}			
		3.50	br	h_0			

[a] Col_h: Hexagonal columnar phase. Cr_X: Partially crystalline solid. I: Isotropic liquid. d_{meas} and d_{calcd} are the measured and calculated diffraction spacing, respectively; d_{calcd} is deduced from the following mathematical expression: $<d_{10}>=1/N_{hk}[\Sigma_{hk}d_{hk}(h^2+k^2+hk)^{1/2}]$, where N_{hk} is the number of hk reflections; I is the intensity of the sharp reflections (vs: very strong, m: medium, w: weak), br stands for broad scattering; hk are the indices of the reflections corresponding to hexagonal 2D symmetry; a is the lattice parameter ($a=2<d_{10}>/\sqrt{3}$), S is the lattice area ($S=a\times<d_{10}>$). The molecular volume was measured for compound **3** and estimated for compound **4** according to: $V_{mol}(\mathbf{4})\sim V_{mol}(\mathbf{3})+V_{DOS}-V_{OTf}$ (see text); h_0, h_{ch}, and h' are the various short-range periodicities determined by X-ray diffraction corresponding to the molecular-stacking distance (h_0), the liquid-like order of the molten chains (h_{ch}), and double periodicity $h'=2h_0$; h is the intracolumnar repeating distance, deduced directly from the measured molecular volume and the columnar cross-section according to $h=V_{mol}/S$. [b] ΔH [kJ mol^{-1}].

ion, remaining the same for both OTf and DOS derivatives. Only a slight expansion of the hexagonal cell was observed with the most voluminous DOS anion ($a=24.8$ Å for compound **3** versus $a=28.0$ Å for compound **4**), increasing the columnar cross-section of the disc. The magnified views in Figure 2 show that the diffraction patterns of compounds **3** and **4** exhibit broad scattering in the wide-angle region. In addition to the typical halo at approximately 4.7 Å (h_{ch}), characteristic of the diffraction of the side chains in their liquid-like order, a scattering diffuse band at about 3.5 Å (h_0), corresponding to the molecular-stacking distance along the disc normal within the column, and another weakly intense halo at 7.0 Å (h') were observed (vide infra).

These data are in agreement with the presence, in both cases, of discrete dimers in which the silver atoms of each molecule are gripped by two triflate (or sulfate) groups in a double-bridged fashion, giving rise to a supramolecular arrangement favorable to a liquid-crystalline assembly (Figure 3).

The so-formed dimers interact with each other along the columns as indicated by the presence of the halo $h'=2h$ centered at 7 Å in the powder XRD spectra.

A similar coordination network observed in bis(phenylthio)propane-[18] and 4-methoxystyrylpyridinatosilver(I)[19] salts was observed in the solid state, in which the effect of a "pincer", such as a coordinating counterion, induces metal–metal distances sufficiently short to be considered as an argentophilic interaction (3.05–3.74 Å). These values are consistent with the stacking periodicity h_0 observed for complexes **3** and **4**. Thus, in the bischelate DOS and OTf derivatives, the counterions force the molecules into a strongly distorted environment, with the Ag^I ions in a geometry closer to the square-planar,[20] in agreement with the formation of strong stacking intra- and interdimers.

Dilatometry experiments were performed on complex **3** to investigate the structural organization of the columns within the mesophase.

From a geometrical point of view, columnar structures are characterized by two parameters: the columnar cross section (S) and the stacking periodicity (h_0) along the molecular-disc normal.[21] The knowledge of these two structural parameters permits the understanding of a specific molecular packing inside the columns and the proposal of models of molecular organizations.[22] The intracolumnar repeating periodicity along the columnar axis, h, the columnar cross section, S, and the molecular volume (V_{mol}) are linked analytically through the relation $h\cdot S=N\cdot V_{mol}$ in which N is the number of molecules within the fraction of the column.[21] While S (and h_0) are obtained directly from the X-ray diffraction data (see Table 1), N is chosen to equal unity as the molecule is disc-like. The molecular volume (V_{mol}) is determined experimentally by dilatometry, whereas h is deduced from both XRD and dilatometry measurements. The comparison of h and h_0 is very informative about the various possible organisations of the disc-like molecules within the column as shown in Figure 4.

Prior to the analysis, the variation of the molecular volume of complex **3** as a function of temperature was monitored. The experiment was carried out, with approximately one gram of compound, between room temperature and about 115 °C, and thus included the Col_h-to-I phase transition (Figure 5).

The temperature dependence of the molecular volume is quasilinear over the entire range of experimental temperatures despite the change from the mesophase to the isotrop-

Figure 1. Optical texture (magnification 40×) of the hexagonal columnar mesophase of compound: a) $[Ag(L^*)_2][OTf]$ (**3**) as observed on cooling at 83 °C; b) $[Ag(L^*)_2][DOS]$ (**4**) as observed on cooling at 31 °C.

ic liquid. From this experiment, the volume of compound **3** varies as $V_{mol} = 1772.7 + 1.341T$ (in Å^3, and T in °C). The slope is in fairly good agreement with the volume variation of the methylene groups in liquid alkanes,[23] an indication that the volume of the rigid part is almost unchanged with temperature in the mesophase. Thus at 30 °C, the volume of complex **3** is equal to about 1810 Å^3. The good reproducibility of the experiment was verified over several heating–cooling cycles (see Supporting Information).

The volume of complex **4** was not measured experimentally but could be estimated from that of complex **3**. Indeed, V_{mol} can be written as a sum of elementary volumes associated with the different segments of the molecule according to $V_{mol} = V_{Core} + V_{Ch}$, whereby V_{Core} and V_{Ch} are the volumes of the rigid core and of the aliphatic chains, respectively. The only difference between the volumes of complexes **3** and **4** is the nature of the counterion, and thus this sum of volumes can be re-written according to $V_{mol}(\mathbf{4}) \sim V_{mol}(\mathbf{3}) + V_{DOS} - V_{OTf}$ where $V_{DOS} = V_{SO_4} + 11V_{CH_2} + V_{CH_3}$, $V_{OTf} = V_{SO_3} + V_{CF_3}$, $V_{CH_2} = 26.5616 + 0.02023T$ (volume of one methylene group), $V_{CH_3} = 53.8221 + 0.03492T + 0.0004258T^2$ (volume of the methyl group), $V_{CF_3} = 68.903 + 0.41998T - 0.0004258T^2$ (volume of one fluoromethyl group). The difference in volume between the sulfate and sulfonate heads is deduced from the difference between the volume of sulfuric acid and sulfurous acid, $\Delta = V_{SO_4} - V_{SO_3} = -43.81$ Å^3. The expression of $V_{mol}(\mathbf{4})$ can be simplified as $V_{mol}(\mathbf{4}) \sim V_{mol}(\mathbf{3}) - \Delta + 11V_{CH_2} + V_{CH_3} - V_{CF_3}$. At 30 °C, $V_{mol}(\mathbf{4}) = 2110$ Å^3. From the V_{mol} of complexes **3** and **4** it is possible to calculate the h values of 3.4 and 3.1 Å, respectively (Table 1).

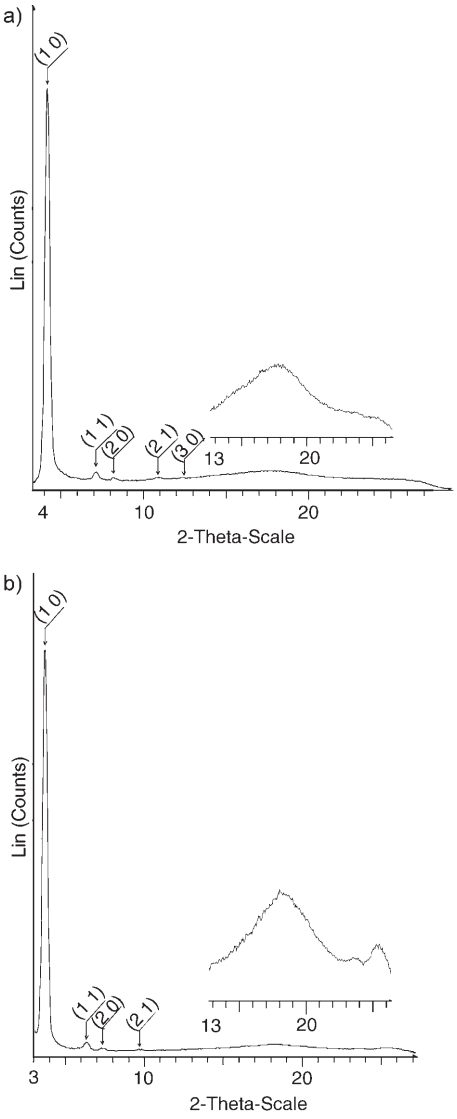

Figure 2. Powder X-ray diffraction patterns of the columnar hexagonal phase at room temperature for complexes **3** (a) and **4** (b).

Figure 3. Sketch of model molecules of complex **3** stacked in a discrete dimer and gripped by two triflate ions.

It can be seen that the stacking distance h_0 is larger, for both cases, than the intracolumnar repeat unit h, particularly in the case of complex **4**, indicating either strong undula-

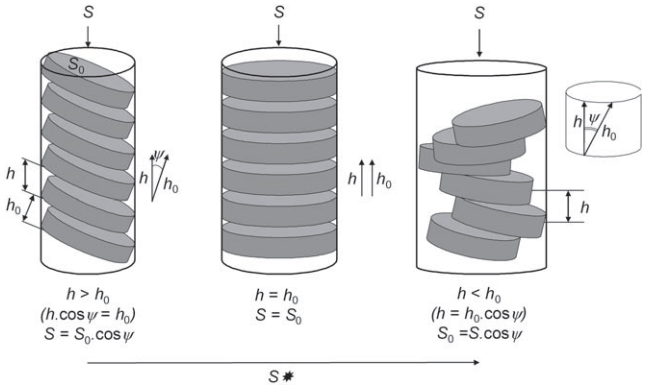

Figure 4. Representation of three types of stacking of discs within the column and the correspondence between the different parameters h, h_0, S, and S_0 (obtained from X-ray diffraction and dilatometry) allowing for their discrimination; ψ is the angle between the columnar axis and the molecular disc normal: Left: The discs are slightly tilted with respect to the columnar axis; middle: The disc normal and columnar axis are perfectly collinear: right: The discs are tilted and arranged in such a way that they precess around the columnar axis (helical packing).

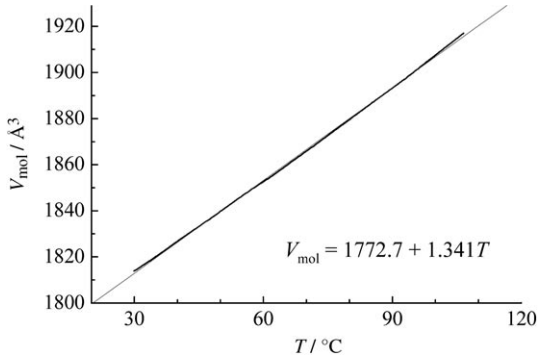

Figure 5. Temperature dependence of the molecular volume of complex **3**.

tions of the columnar cores[24] or helical twisting,[25] about the columnar axis (lateral expansion combined with tilting of the disc, and thus a larger apparent surface area). This result supports the hypothesis of the formation of helical columns (Figure 4, right).

UV/Vis and CD spectra: The UV/Vis absorption and emission spectra of $[Ag(L^*)_2][X]$ were obtained to investigate the role of the chiral centers introduced into the peripheral tails.

The absorption UV/Vis spectra of dilute solutions of compounds **1–4** in dichloromethane exhibited a broad absorption band in the region 250–400 nm, with the maximum centered at around 310 nm and a shoulder in the range 340–380 nm (Table 2).

In analogy to the related achiral compounds previously investigated,[15] the absorptions at high energy are associated with the π–π* electronic transition of the single aromatic chromophores, while the weak n–π* transitions are related to the carboxylic groups.

Table 2. UV/visible absorption maxima of the ligand and solutions of complexes **1–4** in CH_2Cl_2.

Compound	Abs, λ [nm] (ε, [$M^{-1}cm^{-1}$]
L*	241(12400), 300(13900)
1	240(sh), 308(28800)
2	240(sh), 310(26080)
3	240(sh), 311(21800)
4	240(sh), 310 (24200)

However, the analysis of UV/Vis emission spectra showed that the substituents in the 4,4′ positions play a crucial role in the deactivation path of the excited state. Indeed, whereas the silver(I) achiral complexes $[Ag(L^n)_2]X$ were luminescent in solution, showing a maximum at about 350 nm attributable to a ligand-centered transition,[15] no emission was detected for complexes **1–4**, in solution, or for their respective ligand.

The emission properties have been investigated also in pure solid samples at room temperature. Interestingly, while complexes **1** and **2** are not luminescent, complexes **3** and **4**, which are mesomorphic at room temperature, are luminescent, with the lifetime of the excited state lasting less than 30 μs for both complexes (Figure 6 and Table 3).

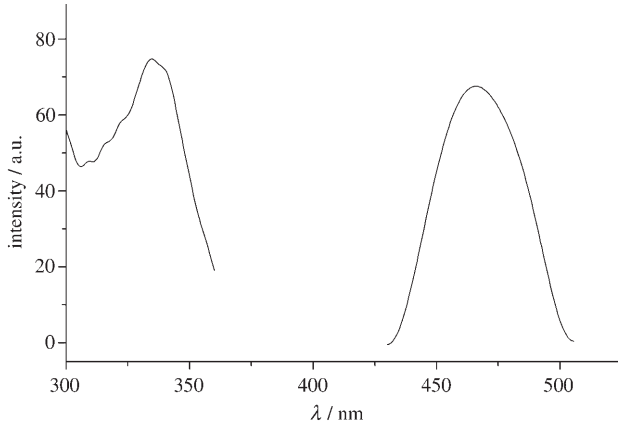

Figure 6. Emission (on the right; $\lambda_{ex} = 330$ nm) and excitation (on the left; $\lambda_{em} = 460$ nm) spectra of compound **3** (neat compound at room temperature).

Table 3. Luminescence data for complexes **3** and **4** in the mesophase, at room temperature.

Compound	Ex, λ [nm]	Em, λ [nm]
3	335	460
4	335	486

The most important features in the photoluminescence emission and excitation spectra of complexes **3** and **4** are the large Stokes shift and the structureless emission band. The observed large Stokes-shifted emission could be attributed to phosphorescence, but the lifetimes exclude a triplet emission. Large Stokes shifts are also indicative of highly

distorted excited states, as reflected in the broadness of the luminescence bands.

These observations proved that the structureless emission arises from an excimer-like[26] organization, only present in the mesomorphic arrangement, since no emission was detected in very concentrated solutions of complexes **3** and **4.** Indeed, in the mesomorphic state the supramolecular arrangement proposed for compounds **3** and **4** can allow the single molecule to be separated by a stacking distance of about 3.5 Å, the typical value found for solid-state excimers and/or exciplexes related to the presence of metal–metal interactions.[27–29]

The presence of four stereogenic centers on each molecule of the $[Ag(L^{*})_2]X$ complexes can confer a formal optical activity derived from the helical organization in the mesophase rather than just the response of the molecular chirality.[12] Thus, circular dichroism (CD) experiments were carried out to confirm this possibility.

The CD spectra of solutions of the OTf and DOS derivatives in dichloromethane displayed similar features: A weak positive dichroic absorption with maxima strictly related to their UV/Vis absorption maximum (Figure 7 and Table 4). No particular differences between absorption wavelengths,

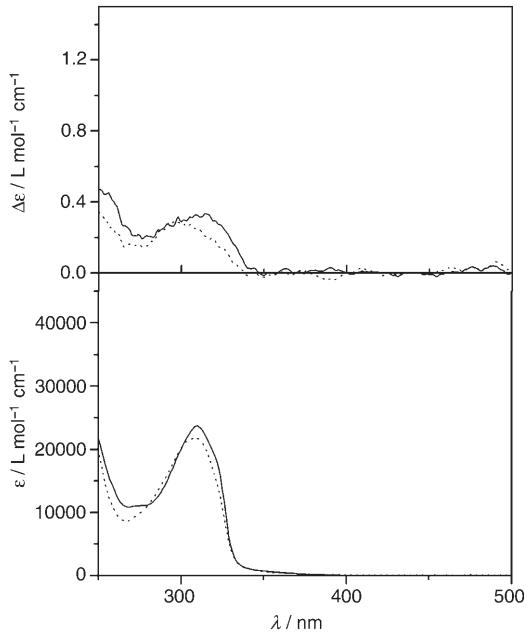

Figure 7. UV/Vis (bottom) and CD (top) spectra of solutions of the complexes **3** (– – –) and **4** (——) in CH_2Cl_2.

Table 4. CD spectra of solutions of complexes **3** and **4** in CH_2Cl_2 at 25 °C.

Sample	CD band	
	λ_{max}[a]	$\Delta\varepsilon_1$[b]
3	300	+0.27
4	310	+0.32

[a] Wavelength [nm] of maximum dichroic absorption. [b] $\Delta\varepsilon$ expressed in $M^{-1}cm^{-1}$.

Cotton effects, and intensity were observed by changing the counterion. It is evident that in dilute solutions (concentration of the complexes approximately 3.0×10^{-4} M) the small circular dichroic behavior of complexes **3** and **4** is attributable to the presence of intrinsic dissymmetry of the *S*-(−)-β-citronellyl unit within the side chains, which induces a chiral perturbation of the electronic transitions.

Thin films were prepared by spin coating the solutions of compounds **3** and **4** onto fused-silica slides. The thickness of the films was regulated to give UV/Vis spectra with maximum absorbance between 0.7–1.0 units, to enable the direct correlation between the properties in the dilute solutions with those exhibited in the mesophase. UV/Vis and CD experiments were performed on these thin solid films (area examined 0.5 cm^2), at room temperature (mesophase) and at 100 °C (isotropic phase). Figure 8 illustrates the CD ellipticity and UV/Vis absorption spectra of both complexes in the mesophase, after isotropization and in dilute dichloromethane solutions.

The CD spectra of the isotropic melt and solution of both complexes exhibited similar Cotton effects of low intensity, while the CD spectra (of both complexes) in the mesomorphic state were very different to those of the complexes in dilute solutions (where the complex molecules are isolated from each other) and in the isotropic state.

The CD spectrum of the thin film of compound **3** at room temperature revealed an intense broad circular dichroism in the 280–400 nm spectral region, characterized by two negative CD peaks with maxima at 321 and 330 nm and a weak positive dichroic band at 300 nm, (Figure 8a). No significant CD bands were visible in the dilute solution and the isotropic sample of compound **3**. The CD spectrum of compound **4** (Figure 8b) in its mesomorphic state is quite similar to that of compound **3** but a positive broad and weak dichroic signal is visible, centered at around 375 nm, which could be due to the weak n–π* transition of carboxylic groups as observed in the solid-state UV/Vis spectrum.

In the CD spectra of compounds **3** and **4**, the overlapping of several CD signals, which is correlated with electronic transitions (see UV/Vis transitions present in solution and described in the previous section) in the 250–400 nm spectrum region, may be responsible for a slight shift in the Cotton-effect bands with respect to the corresponding UV/Vis maximum absorption, preventing the full identification of every CD peak.

In addition, an exciton splitting of low intensity for complex **3**, and of higher intensity for complex **4**, is present as indicated by two bands of opposite signs with a crossover point at the same wavelength of the relative UV/Vis electronic transition, nevertheless we observe a partial overlapping with other dichroic signals correlated with several electronic transitions.

However, since the presence of a long alkyl chain in the DOS counterion of complex **4** slightly modifies the columnar cross-section of the disc with respect to complex **3**, as evidenced by the X-ray diffraction measurements, their CD spectra are similar but not perfectly superimposable.

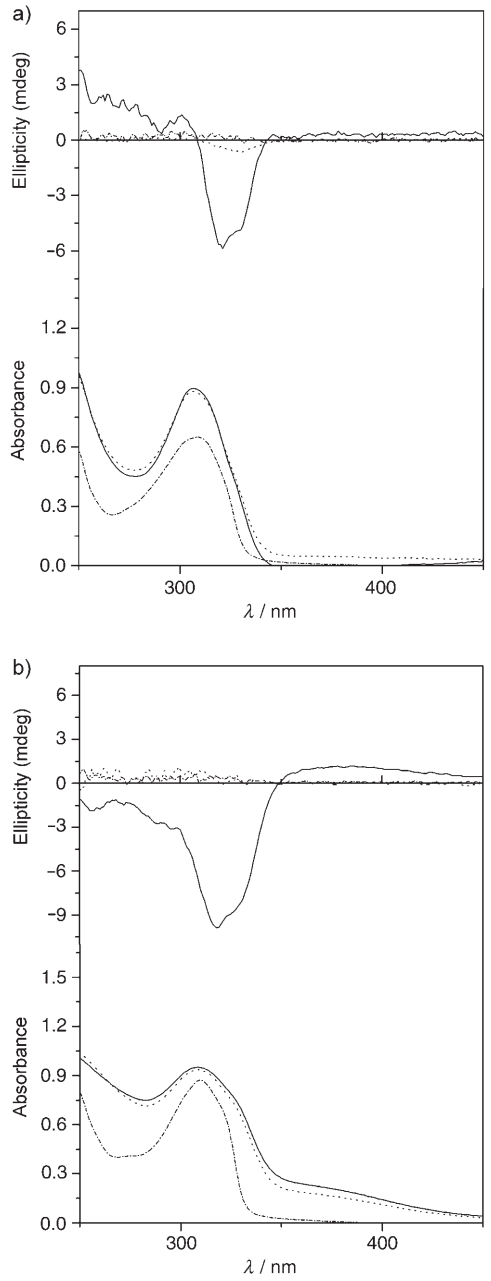

Figure 8. UV (lower) and CD (upper) spectra of **3** (a) and **4** (b) under different conditions: Diluted solution in CH_2Cl_2 (–•–•), thin film in the mesophase at 25 °C (——), and in the isotropic phase at 100 °C (– – –).

Since the appearance of supramolecular chirality in columnar structures can be obtained by different mechanisms[7,25] other than the presence of stereogenic centers, such as the molecular shape and modes of aggregation,[30] analogous CD experiments were performed on the achiral $[Ag(L^n)_2][X]$ complexes in their mesomorphic state, to clarify the nature of the conformational chiral aggregation in the columnar mesophase in these systems. In these cases, no circular dichroism was observed. Therefore the optical activity manifested by complexes **3** and **4** in the mesophase reflects the formation of a supramolecular helical arrangement of the whole columns as a result of the four stereogenic centers in each molecule.

Stability of the helical arrangement was confirmed as the CD spectra obtained on anisotropic films stored for six months at room temperature were comparable to those originally obtained, indicating that the conformational arrangement in the liquid-crystalline state is stable over time and does not undergo further structural changes.

Conclusion

We have synthesized a new, chiral non-mesomorphic 2,2′-bipyridine, L*, and the corresponding bischelate ionic silver(I) complexes $[Ag(L^*)_2][X]$. Mesomorphism is observed only for those derivatives containing coordinating counterions such as OTf and DOS, compounds **3** and **4**, respectively.

Therefore the coordinating ability of these counterions can induce a supramolecular arrangement in which two bischelate cations are connected by two triflate (or sulfate) groups, in a double-bridged fashion, through Ag–O interactions, giving rise to discrete dimers or infinite polymers (Figure 3). The resulting supramolecular arrangement will favour a liquid-crystalline assembly that would otherwise be prevented by the molecular shape of the $[Ag(L^*)_2][X]$ complexes.

X-ray diffraction investigations on complexes **3** and **4** confirmed the formation of the room-temperature hexagonal columnar phases initially observed by POM analysis. Moreover, volume measurements in the mesomorphic state indicate helical twisting about the columnar axis and support the hypothesis of the formation of helical columns. To confirm these results CD experiments were performed in solution and on the liquid crystalline films of compounds **3** and **4.** From these data we can confirm that, in these systems, chirality is induced from the single-molecule level to a supramolecular columnar liquid-crystalline organization. Therefore, the supramolecular arrangement achieved gives rise to a helical structure formed by the entire molecular columns in the mesophase.

Finally, the photophysical characterization of compounds **3** and **4** has pointed out that these complexes are luminescent, at room temperature, in their mesomorphic state, and this behavior is very promising for applications as light-emitting diodes. In fact, very few metallomesogens that are luminescent in the mesophase have been reported up to now (lanthanide-based columnar and gold calamitic mesogens)[31–32] but none of them show mesomorphism and luminescence at room temperature.

Moreover the blue luminescence exhibited in the mesophase by compounds **3** and **4** is not usual and can be ascribed to the existence of excimers arising from argentophilic interactions that are intradimeric within the columns.

The synthetic strategy based on several construction motifs has been useful to synthesize materials the properties of which can be properly and finely modulated through the specific intermolecular interactions. Indeed, in this class of

complexes, we have several construction motifs with a variety of possible molecular and intermolecular organizations. Both bipyridines and the silver(I) ion are versatile systems that can lead to different structures depending on coordination modes, solvent, reaction conditions, and nature of anions. In the case of the $[Ag(L^*)_2][X]$ compounds, the tetracoordination is achieved through bischelation of two bipyridine units around the silver center. The network formation is then controlled by the choice of the counterion that is the first step towards a supramolecular organization essential to generate, at the same time, room-temperature columnar hexagonal mesomorphism, columnar helical supramolecular structure, and excimeric emission.

Experimental Section

General information: All reagents were used as received from the respective suppliers: 4,4′-dimethyl-2,2′-bipyridine, silver tetrafluoroborate, silver hexafluorophosphate, silver trifluoromethanesulfonate, silver nitrate, sodium dodecylsulfate from Aldrich, and *S*-(−)-β-citronellol from Fluka. Likewise the solvents were used as received from commercial sources without further purification and were dried by using standard methods wherever necessary. The synthesis of 4,4′-dicarboxy-2,2′-bipyridine (**I**) was performed as previously reported.[17] Thin films were prepared by spin coating solutions of samples in CH_2Cl_2 (2% w/w) onto clean fused-silica substrates. Films were then dried under vacuum at 25°C overnight to eliminate any residual solvent. Film thickness was regulated to allow for maximum UV/Vis spectral absorbance between 0.7–1.2 units, depending on the conditions, to enable the direct correlation between the properties of the complexes in thin films and in dilute solutions. As sample thicknesses ranged between 100–200 nm the extinction coefficient and ellipticity values could be considered negligible for the spectra of bulk samples.

^{1}H NMR solution spectra were acquired on a Bruker Avance DRX-300 spectrometer in $CDCl_3$ and [D$_6$]DMSO, with TMS as internal standard. IR spectra were obtained on a Spectrum One FTIR Perkin–Elmer spectrophotometer by using the KBr disc method. Elemental analyses were carried out with a Perkin–Elmer 2400 analyser. The textures of the mesophases were studied with a Zeiss Axioscope polarising microscope equipped with a Linkam CO 600 heating stage. The transition temperatures and enthalpies were measured by using a Perkin–Elmer DSC 6 Differential Scanning Calorimeter with a heating and cooling rate of 10°C min^{-1}. The apparatus was calibrated with indium. At least two heating–cooling cycles were performed on each sample. The powder X-ray diffraction patterns were obtained by using a Bruker AXS General Area Detector Diffraction System (D8 Discover with GADDS) with $Cu_{K\alpha}$ radiation; The highly sensitive area detector was placed at a distance of 20 cm from the sample and at an angle $2\theta_D$ of 12°. A CalCTec (Italy) variable heating stage was used to heat the samples at a rate of 5.0°C min^{-1} to the appropriate temperature. Measurements were performed by charging samples in Lindemann capillary tubes with inner diameters of 0.5 mm.

A Perkin–Elmer Lambda 19 UV/Vis spectrophotometer was used to record absorption spectra on solutions in CH_2Cl_2 at 25°C in the 700–240 nm spectral region by using cell path lengths of 0.1 cm. Concentrations of 3.0×10^{-4} and 3.7×10^{-4} mol L^{-1} of compounds **3** and **4**, respectively, were used. These compounds are fairly stable in dichloromethane, as demonstrated by the constancy of their absorption spectra over a week. CD spectra were recorded at 25°C at a scanning speed of 50 nm min^{-1} on a Jasco 810 A dichrograph, by using the same path lengths and solution concentrations as for UV/Vis measurements. $\Delta\varepsilon$ values, expressed as L mol^{-1} cm^{-1}, were calculated by using the following equation: $\Delta\varepsilon=[\Theta]/3300$ where the molar ellipticity $[\Theta]$ is expressed in deg cm^2 dmol^{-1}. To avoid linear effects (linear dichroism and linear birefringence) due to orientation anisotropy in the ordered systems, several CD spectra were recorded as the sample in the thin-film state was rotated through successive 60° increments around the light source. The temperature was maintained constant by using a plate holder.[33–36] The UV/Vis and CD spectra did not change significantly so averaged spectra were used for the analysis.

Spectrofluorimetric grade dichloromethane (Acros Organics) was used for investigating the photophysical properties of the complexes in solution at room temperature. Neat compounds were examined on a quartz window. A Perkin–Elmer Lambda 900 spectrophotometer was employed to measure the absorption spectra, while the corrected emission spectra, all confirmed by excitation spectra, were recorded with a Perkin–Elmer LS 50B spectrofluorimeter, equipped with a Hamamatsu R928 photomultiplier tube.

Dicitronellyl 2,2′-bipyridyl-4,4′-dicarboxylate (L*): A mixture of 4,4′-dicarboxy-2,2′-bipyridine, **I**, (0.50 g, 0.96 mmol) and thionyl chloride (19 mL) were refluxed under nitrogen until a clear yellow solution was obtained. Excess thionyl chloride was removed and the residue was dried under vacuum for 2 h. Acid chloride **II** was suspended in toluene (20 mL) and treated with a slight excess of *S*-(−)-β-citronellol (0.90 mL, 4.91 mmol). The mixture was heated under reflux for 3 h. The solvent was evaporated before the addition of chloroform (40 mL) and the mixture was washed with a solution of saturated sodium hydrogen carbonate (40 mL). The aqueous layer was then rigorously mixed in chloroform (3× 15 mL). The organic extract was washed with water (100 mL), dried over anhydrous sodium sulfate, filtered, and evaporated to dryness. The pure product was obtained by chromatography by using the solvent mixture dichloromethane/diethyl ether (9:1) as elution medium. Evaporation of the solvent gave a yellowish oil in a 78% yield. IR (KBr): $\tilde{\nu}=1730$ cm^{-1} (C=O); ^{1}H NMR (300 MHz, $CDCl_3$): $\delta=8.94$ (s, 2H; H$^{3,3'}$), 8.87 (d, $^3J=4.7$ Hz, 2H; H$^{6,6'}$), 7.90 (dd, $^3J=4.7$ Hz and $^4J=1.7$ Hz, 2H; H$^{5,5'}$), 5.10 (m, 2H; H$^{b,b'}$), 4.43 (m, 4H; H$^{h,h'}$), 2.01 (m, 4H; H$^{c,c'}$), 1.87 (m, 2H; H$^{e,e'}$), 1.64 (m, 12H; H$^{a,a'}$), 1.33 (m, 8H; H$^{d,d',g,g'}$), 0.99 ppm (d, $^3J=6.0$ Hz, 6H; H$^{f,f'}$); $C_{32}H_{44}N_2O_4$ (520.71).

General procedure for the synthesis of silver complexes $[Ag(L^*)_2][X]$: A solution of dicitronellyl 2,2′-bipyridyl-4,4′-dicarboxylate (0.365 mmol) in dichloromethane (10 mL) was added to a stirred suspension of silver(I) salt (0.183 mmol) in dichloromethane (10 mL) and the mixture was heated under reflux for 24 h. The solvent was evaporated and the residue recrystallized from methanol.

(2,2′-bipyridyl-4,4′-bis-citronellylcarboxylate)silver(I)tetrafluoroborate, (**1**): Yellow oil. Yield 47%. IR (KBr): $\tilde{\nu}=1730.6$ (C=O), 1066.9 cm^{-1} (BF_4); ^{1}H NMR (300 MHz, $CDCl_3$): $\delta=8.93$ (d, $^3J=5.1$ Hz, 4H; H$^{6,6'}$), 8.82 (s, 4H; H$^{3,3'}$), 8.12 (d, $^3J=5.1$ Hz, 4H; H$^{5,5'}$), 5.11 (t, $^3J=7.0$ Hz, 4H; H$^{b,b'}$), 4.49 (t, $^3J=6.2$ Hz, 8H; H$^{h,h'}$), 2.02 (m, 8H; H$^{c,c'}$), 1.89 (m, 4H; H$^{e,e'}$), 1.64 (m, 24H; H$^{a,a'}$), 1.37 (m, 16H; H$^{d,d',g,g'}$), 1.01 ppm (d, $^3J=6.0$ Hz, 12H; H$^{f,f'}$); $AgBC_{64}F_4H_{88}N_4O_8$ (1236.10).

(2,2′-bipyridyl-4,4′-bis-citronellylcarboxylate)silver(I)hexafluorophosphate, (2): Yellow solid. Yield 64%. Mp 60.6°C. IR (KBr): $\tilde{\nu}=1730.8$ (C=O), 832.1 cm^{-1} (PF_6); ^{1}H NMR (300 MHz, $CDCl_3$): $\delta=8.88$ (d, $^3J=4.7$ Hz, 4H; H$^{6,6'}$), 8.82 (s, 4H; H$^{3,3'}$), 8.13 (d, $^3J=5.1$ Hz, 4H; H$^{5,5'}$), 5.11 (m, 4H; H$^{b,b'}$), 4.50 (t, $^3J=6.2$ Hz, 8H; H$^{h,h'}$), 2.03 (m, 8H; H$^{c,c'}$), 1.90 (m, 4H; H$^{e,e'}$), 1.65 (m, 24H; H$^{a,a'}$), 1.37 (m, 16H; H$^{d,d',g,g'}$), 1.01 ppm (d, $^3J=6.4$ Hz, 12H; H$^{f,f'}$); elemental analysis calcd (%) for $AgC_{64}F_6H_{88}N_4O_8P$ (1294.26): C 59.39, H 6.85, N 4.33; found: C 59.23, H 6.76, N 4.31.

(2,2′-bipyridyl-4,4′-bis-citronellylcarboxylate)silver(I)trifluoromethanesulfonate, (3): Yellow wax. Yield 73%. Thermotropic behavior shown in Table 1. IR (KBr): $\tilde{\nu}=1730.5$ (C=O), 1285.8 (OTf), 1254.9 cm^{-1} (OTf); ^{1}H NMR (300 MHz, $CDCl_3$): $\delta=8.93$ (d, $^3J=5.1$ Hz, 4H; H$^{6,6'}$), 8.78 (s, 4H; H$^{3,3'}$), 8.08 (d, $^3J=4.9$ Hz, 4H; H$^{5,5'}$), 5.11 (m, 4H; H$^{b,b'}$), 4.49 (t, $^3J=6.2$ Hz, 8H; H^{h,h}), 2.01 (m, 8H; H$^{c,c'}$), 1.89 (m, 4H; H$^{e,e'}$), 1.66 (m, 24H; H$^{a,a'}$), 1.35 (m, 16H; H$^{d,d',g,g'}$), 1.01 ppm (d, $^3J=6.4$ Hz, 12H; H$^{f,f'}$); elemental analysis calcd (%) for $AgC_{65}F_3H_{88}N_4O_{11}S$ (1298.36): C 60.13, H 6.83, N 4.32; found: C 59.52, H 6.83, N 4.34.

(2,2′-bipyridyl-4,4′-bis-citronellylcarboxylate)silver(I)dodecylsulfate, (4): Yellow wax. Yield 37%. Thermotropic behavior shown in Table 1. IR (KBr): $\tilde{\nu}=1730.1$ (C=O), 1255.9 (DOS), 1220 cm^{-1} (DOS); ^{1}H NMR (300 MHz, [D$_6$]DMSO): $\delta=8.95$ (d, $^3J=4.9$ Hz, 4H; H$^{6,6'}$), 8.83 (s, 4H; H$^{3,3'}$), 7.94 (d, $^3J=4.9$ Hz, 4H; H$^{5,5'}$), 5.10 (m, 4H; H$^{b,b'}$), 4.43 (m, 8H; H$^{h,h'}$), 3.69 (t, $^3J=6.6$ Hz, 2H; CH_2 of DOS), 1.98 (m, 8H; H$^{c,c'}$), 1.81 (m,

4H; $H^{e,e'}$), 1.66 (m, 26H; $H^{a,a'}$, CH_2 of DOS), 1.40 (m, 16H; $H^{d,d',g,g'}$), 1.25 (m, 18H; CH_2 of DOS), 0.96 (d, $^3J = 6.4$ Hz, 12H; $H^{f,f'}$), 0.85 ppm (t, $^3J = 6.8$ Hz, 3H; CH_2 of DOS); elemental analysis calcd (%) for $AgC_{76}H_{113}N_4O_{12}S$ (1414.68): C 64.53, H 8.05, N 3.96; found: C 64.97, H 8.09, N 4.16.

Acknowledgements

This work was partly supported by grants from the Italian Ministero dell'Istruzione, dell'Università e della Ricerca (MIUR) through the INSTM-FIRB RBNE01P4JF, MIUR PRIN2004 and Centro di Eccellenza CE-MIF.CAL. B.D. and E.I.S. gratefully thank Dr. Benoît Heinrich for his help in the dilatometry experiment and fruitful discussions.

[1] R. J. Bushby, O. R. Lozman, *Curr. Opin. Colloid Interface Sci.* **2002**, *7*, 343–354.
[2] M. O'Neill, S. Kelly, M. *Adv. Mater.* **2003**, *15*, 1135–1146.
[3] J. Hanna, *Opto-Electron. Rev.* **2005**, *13*, 259–267.
[4] K. Binnemans, *Chem. Rev.* **2005**, *105*, 4148–4204.
[5] R. J. Bushby, O. R. Lozman, *Curr. Opin. Sol. State Mater. Sci.* **2002**, *6*, 569–578.
[6] S. Kumar, *Chem. Soc. Rev.* **2006**, *35*, 83–109.
[7] H.-S. Kitzerow, C. Bahr in *Chirality in Liquid Crystals*, Springer, New York, **2001**.
[8] J. Malthête, J. Jacques, N. H. Tinh, C. Destrade, *Nature* **1982**, *298*, 46–48.
[9] H. Bock, W. Helfrich, *Liq. Cryst.* **1992**, *12*, 697–703.
[10] G. Scherowsky, X. H. Chen, *J. Mater. Chem.* **1995**, *5*, 417–421.
[11] G. Heppke, D. Krüerke, M. Müller, H. Bock, *Ferroelectrics* **1996**, *179*, 203–209.
[12] J. L. Serrano, T. Sierra, *Coord. Chem. Rev.* **2003**, *242*, 73–85.
[13] T. Kato, N. Mizoshita, K. Kishimoto, *Angew. Chem.* **2006**, *118*, 44–74; *Angew. Chem. Int. Ed.* **2006**, *45*, 38–68.
[14] D. Pucci, G. Barberio, A. Crispini, O. Francescangeli, M. Ghedini, *Mol. Cryst. Liq. Cryst.* **2003**, *395*, 155–165.
[15] D. Pucci, G. Barberio, A. Bellusci, A. Crispini, M. La Deda, M. Ghedini, E. Szerb, *Eur. J. Inorg. Chem.* **2005**, 2457–2463.
[16] G. Barberio, A. Bellusci, A. Crispini, M. Ghedini, A. Golemme, P. Prus, D. Pucci, *Eur. J. Inorg. Chem.* **2005**, 181–188.
[17] D. W. Bruce, K. E. Rowe, *Liq. Cryst.* **1995**, *18*, 161–163.
[18] M. O. Awaleh, A. Badia, F. Brisse, *Inorg. Chem.* **2005**, *44*, 7833–7845.
[19] H. Adams, N. A. Bailey, D. W. Bruce, S. C. Davis, D. A. Dunmur, P. D. Hempstead, S. A. Hudson, S. Thorpe, *J. Mater. Chem.* **1992**, *2*, 395–400.
[20] E. C. Constable, C. E. Housecroft, B. M. Kariuki, M. Neuburger, C. B. Smith, *Aust. J. Chem.* **2003**, *56*, 653–655.
[21] D. Guillon, *Struct. Bonding (Berlin)* **1999**, *95*, 41–82.
[22] a) F. Morale, R. W. Date, D. Guillon, D. W. Bruce, R. L. Finn, C. Wilson, A. J. Blake, M. Schröder, B. Donnio, *Chem. Eur. J.* **2003**, *9*, 2484–2501; b) B. Donnio, B. Heinrich, H. Allouchi, J. Kain, S. Diele, D. Guillon, D. W. Bruce, *J. Am. Chem. Soc.* **2004**, *126*, 15258—15268.
[23] A. K. Doolittle, *J. Appl. Phys.* **1951**, *22*, 1471–1475.
[24] B. Donnio, B. Heinrich, T. Gulik-Krzywicki, H. Delacroix, D. Guillon, D. W. Bruce, *Chem. Mater.* **1997**, *9*, 2951–2965.
[25] J. L. Serrano, T. Sierra, *Chem. Eur. J.* **2000**, *6*, 759–766.
[26] a) T. H. Lowry, K. Schuller-Richardson in *Mechanism and Theory in Organic Chemistry*, Harper & Row, New York, **1981**; b) N. J. Turro in *Modern Molecular Photochemistry*, Benjamin/Cummings, Menlo Park, CA, **1978**; c) A. A. Lamola in *Energy Transfer and Organic Photochemistry* (Eds.: A. A. Lamola, N. J. Turro), Wiley-Interscience, New York, **1969** d) M. Gordon, W. R. Ware in *The Exciplex*, (Eds.: M. Gordon, W. R. Ware), Academic Press, New York, **1975**; e) J. Kopecky in *Organic Photochemistry: A Visual Approach*, VCH, New York, **1991**; f) J. Michl, V. Bonacic-Koutecky in *Electronic Aspects of Organic Photochemistry*, Wiley, New York, **1990**, pp. 274–286.
[27] a) S. A. Clodfelter, T. M. Doede, B. A. Brennan, J. K. Nagle, D. P. Bender, W. A. Turner, P. M. LaPunzina, *J. Am. Chem. Soc.* **1994**, *116*, 11379–11386; b) J. K. Nagle, B. A. Brennan, *J. Am. Chem. Soc.* **1988**, *110*, 5931–5932.
[28] K. R. Kylie, P. C. Ford, *J. Am. Chem. Soc.* **1989**, *111*, 5005–5006.
[29] a) M. A. Omary, H. H. Patterson, *Inorg. Chem.* **1998**, *37*, 1060–1066; b) M. A. Omary, H. H. Patterson, *J. Am. Chem. Soc.* **1998**, *120*, 7696–7705.
[30] a) R. A. Reddy, C. Tschierske, *J. Mater. Chem.* **2006**, *16*, 907–961; b) H. M. Keizer, R. P. Sijbesma, *Chem. Soc. Rev.* **2005**, *34*, 226–234.
[31] S. Suàrez, D. Imbert, F. Gumy, C. Piguet, J.-C. G. Bunzli, *Chem. Mater.* **2004**, *16*, 3257–3266.
[32] R. Bayon, S. Coco, P. Espinet, *Chem. Eur. J.* **2005**, *11*, 1079–1085.
[33] J. Schellmann, H. P. Jensen, *Chem. Rev.* **1987**, *87*, 1359–1367.
[34] A. Hans-Werner, S. Dähne, A. Ouart, C. Spitz, *J. Phys. Chem. B* **2000**, *104*, 8664–8669.
[35] L. Angiolini, R. Bozio, L. Giorgini, D. Pedron, G. Turco, A. Daurû, *Chem. Eur. J.* **2002**, *8*, 4241–4247.
[36] A. Rodger, B. Norden in *Circular Dichroism and Linear Dichroism*, Oxford University Press, Oxford, **1997**.

Received: March 23, 2006
Published online: July 21, 2006

